

Interpretative analysis of particle confinement time on MAST

G P Maddison, A Turner, M Valovič

EURATOM/UKAEA Fusion Association,
Culham Science Centre, Abingdon, Oxon. OX14 3DB, UK.

1. Introduction

In contrast to analysis of global energy balance, majority-ion confinement time on tokamaks is usually obscured by the difficulty of determining source rates, which are a complicated blend of direct inputs and pumping with recycling. A total quantity τ_p (s) may be expressed :-

$$\frac{dN_i^{\text{tot}}}{dt} = -\frac{N_i^{\text{tot}}}{\tau_p} + S = -\frac{N_i^{\text{tot}}}{\tau_p^*} + S_{\text{add}} \quad \sim \quad \frac{dN_i}{dt} = -\frac{N_i}{\tau_i} + e_1^{\text{recycle}} S_{\text{recycle}} + e_1^{\text{add}} S_{\text{add}} \quad ,$$

where N_i^{tot} is the total fuel-ion content and $N_i \sim N_i^{\text{tot}}$ is their number within the confined region; $S \equiv S_{\text{recycle}} + S_{\text{add}}$ (s^{-1}) is total source rate consisting of recycling and externally-added components respectively; $0 \leq e_1 \leq 1$ are efficiencies with which these contribute to the core plasma; and $\tau_i \sim a^2/D_{\perp}$ is consequently a time more representative of diffusion across this zone. When all added fuelling is switched off ($S_{\text{add}} = 0$), N_i^{tot} cannot decline faster than net effective confinement time $\tau_p^* = \tau_p / (1 - R) \geq \tau_p$, where $0 \leq R \equiv \tau_p S_{\text{recycle}} / N_i^{\text{tot}} \leq 1$ is an overall recycling coefficient. Similarly :-

$$\tau_i \sim \tau_p^* \frac{N_i}{N_i + \tau_p^* [e_1^{\text{recycle}} S_{\text{recycle}} - (1 - e_1^{\text{add}}) S_{\text{add}}]} \sim \tau_p \frac{N_i}{N_i - \tau_p [(1 - e_1^{\text{recycle}}) S_{\text{recycle}} + (1 - e_1^{\text{add}}) S_{\text{add}}]} \geq \tau_p \cdot$$

Derivation of τ_i requires a sufficiently detailed description of particle input, effluxes and recycling. A global model adapted for the large ratio of vessel to plasma volumes ($\sim 10 : 1$) on MAST has been developed^[1], in particular distinguishing between molecular and atomic processes and allowing for an extended gas envelope around the plasma fed directly by outboard puffing. An initial survey of discharges with such input has been undertaken, by adjusting for each one both model τ_i and wall recycling coefficient as functions of time in order to match experimental signals for volume-average electron density $\langle n_e \rangle$ (m^{-3}) and estimated global $\text{D}\alpha$ emission $4\pi A_p \zeta_{\text{D}\alpha} \approx \{ \Gamma_1^{\text{D}} / (\text{S/XB})^{\text{D}} + \Gamma_1^{\text{D}2} / (\text{“S/XB”})^{\text{D}2} \}$. Here A_p (m^2) is the separatrix surface area, $\zeta_{\text{D}\alpha}$ ($\text{photons m}^{-2} \text{sr}^{-1} \text{s}^{-1}$) is main-plasma $\text{D}\alpha$ radiance, Γ_1 (s^{-1}) are ionizing fluxes of respective neutral particles, and ratio of atomic rate coefficients^[2] $(\text{S/XB})^{\text{D}} \approx 14$. One issue is that effective molecular emission factor $(\text{“S/XB”})^{\text{D}2}$ does not reduce to such a simple number owing to terms proceeding first through molecular ionization ($e^- + \text{D}_2 \rightarrow 2e^- + \text{D}_2^+$). Sensitivity to this parameter is considered in following results.

2. Core deuteron confinement time τ_i

A sample of 67 MAST outboard-puffed plasmas has been modelled, comprising mainly double-null-diverted with some centre-column-limited cases, while encompassing both Ohmic and neutral-beam-heated operation. Gas inputs were separately calibrated using a validated ionization gauge for injection into the vessel with no plasma or fields applied. Core fuelling efficiencies e_1 crucially represent neutral-particle penetration across the separatrix, but become distinguishable^[1] since they affect absolute $\langle n_e \rangle$ most, whereas $\partial \langle n_e \rangle / \partial t$ is more sensitive to τ_i .

Over the ranges examined, $e_1^{\text{recycle}} = e_1^{\text{add}} = 0.1$ were found to be adequate throughout, perhaps consistent with fuelling always from the tank reservoir. Good matches to observed $\langle n_e \rangle(t)$, $4\pi A_p(t)\zeta_{D\alpha}(t)$ were then found to be possible by adapting $\tau_i(t)$ plus just atomic desorption coefficient $\rho_{dD}(t)$, ie each atom striking wall surfaces has a probability $0 \leq \rho_{dD} \leq 1 - \rho_{rD}$ of returning as half of a thermal molecule, where reflection coefficient $\rho_{rD} = 0.5$ (and similarly for ions $\rho_{di} = \rho_{ri} = 0.5$) is assumed^[1]. In the absence presently of active sinks on MAST, pumping is therefore simulated by the fraction $1 - \rho_{rD} - \rho_{dD}$ of atoms adsorbed at the walls. Initially (“S/XB”)^{D2} \approx (S/XB)^D has also been adopted, as suggested in other recent studies^[3], but primarily because this implies minimum possible molecular density in the vacuum tank n_{D2} (m⁻³), thus upper bounds on τ_i and persistence of wall sinks.

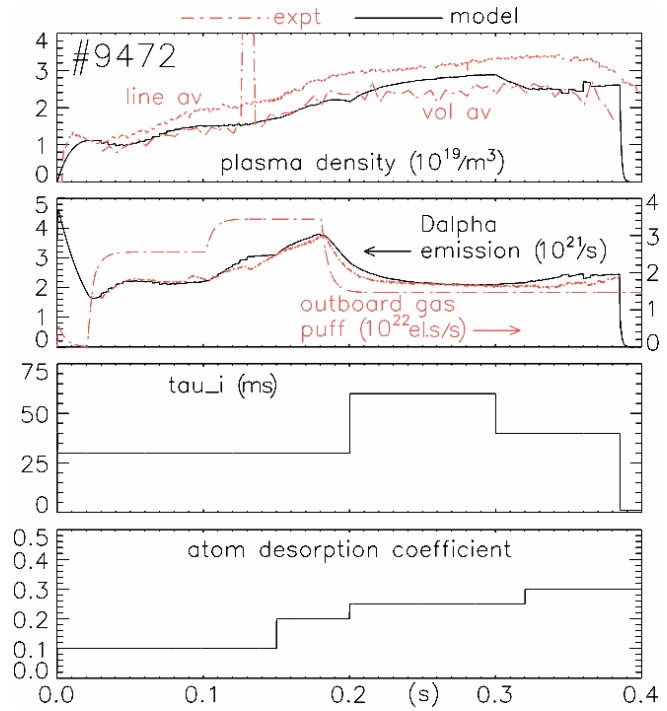


Fig.1 Example model fit to experiment for a MAST Ohmic DND plasma ($e_1 = 0.1$ and assuming (“S/XB”)^{D2} \approx (S/XB)^D).

A typical calculation is shown in Fig.1, actually an Ohmic DND discharge. The sudden step-down of gas puffing Φ_{out} (electrons s⁻¹) at 0.18 s in this instance provokes a rapid rise in particle confinement, illustrating that generally τ_i tends to be highest when fuelling is lowest, and vice versa. In complete gas turn-off experiments τ_i can even become arbitrarily large, as plasma density is sustained for very small sources, so that its value is only defined with substantial uncertainty. These 3 such plasmas are consequently excluded from subsequent regressions. Principal-component analysis over the whole remaining dataset finds strong correlations between computed n_{D2} , line-average electron density \bar{n}_e (m⁻³), and Φ_{out} , so only one of these can be chosen as a regressor; \bar{n}_e is also anti-correlated with confined plasma volume V_p (m³). Furthermore magnetic field B_t (T) varies too little for any dependence upon it to be identified. For the NBH cases alone, which were all in L-mode with auxiliary power P_{NB} (MW), Φ_{out} exhibits almost exact anti-correlation with plasma current I_p (kA). Taking these restrictions into account, regressions separately on the (37) Ohmic and (27) NBH results during steadiest phases yield :-

$$\tau_i^{(\text{Ohmic})} \text{ (ms)} \approx 3.2 \times 10^{12} I_p^{-0.11} V_p^{0.85} \Phi_{\text{out}}^{-0.50} ; \tau_i^{(\text{NBH})} \text{ (ms)} \approx 3.5 \times 10^{21} P_{\text{NB}}^{-0.32} V_p^{0.53} \Phi_{\text{out}}^{-0.91} \quad (e_1 = 0.1).$$

Interestingly these recall the negative current and power dependencies of neo-Alcator and L-mode energy confinement time τ_E respectively. However, an equally large fraction of the variance over all (64) cases, irrespective of heating scheme or configuration, is removed by the single variable fit :-

$$\tau_i \text{ (ms)} \approx 5.3 \times 10^{14} n_{D2}^{-0.70} \quad (e_1 = 0.1),$$

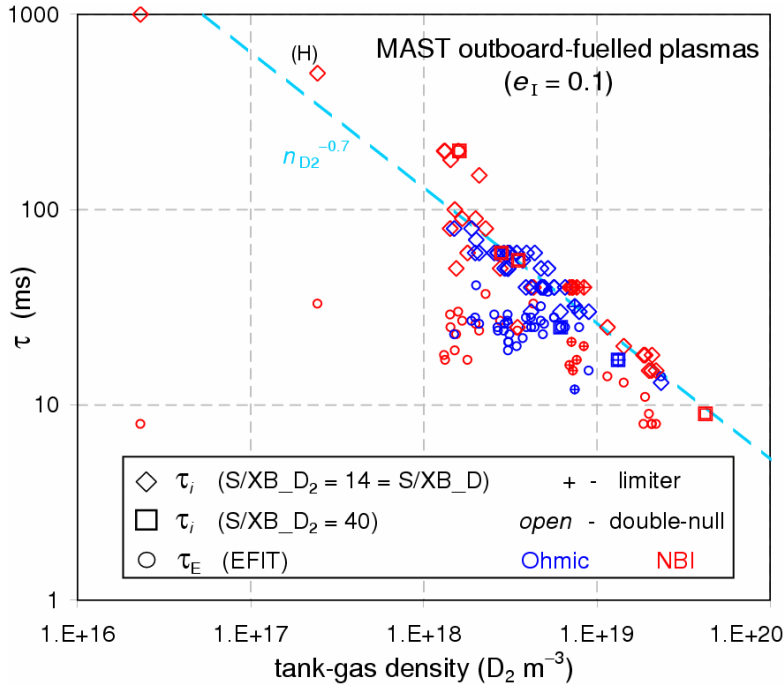


Fig.2 Variation of calculated particle (and energy) confinement time with n_{D2} over all cases. (Instances ≥ 500 ms not included in regression (dashed line). Labelled point is the single H-mode modelled so far.)

3. Wall pumping

In Fig.1 a monotonic rise of inferred $\rho_{dD}(t)$ throughout the pulse is seen, which is typical of results obtained. This is consistent with expected depletion of wall sinks as adsorbed wall inventory $N_w(t)$ (atoms m^{-2}) accumulates. Starting value ρ_{dD0} (N_{w0}) at $t=0$ is roughly inversely correlated with the duration of prior inter-shot helium-glow-discharge cleaning, but depends also on the history (density, power) of immediately preceding discharges. Plotting $\rho_{dD}(t)$ against computed^[1] $N_w(t)$, exemplified for a selection of results in Fig.3, hence allows maximum capacity $N_{wc} \geq N_w(t)$ setting the point at which pumping runs out ($\rho_{dD} = 1 - \rho_{rD} = 0.5$) to be deduced. Saturation of wall sinks broadly indicates a linear rise of desorption :-

$$\rho_{dD}(N_w) \approx \rho_{dD0} + (1 - \rho_{rD} - \rho_{dD0}) \frac{N_w - N_{w0}}{N_{wc} - N_{w0}},$$

which would actually imply available surface sites are occupied by impinging atoms at the greatest rate possible^[1]. In MAST, regular boronization with trimethylborane is used to improve surface conditioning, such that adsorbing layers consist largely of an amorphous mixture of carbon and boron. From Fig.3, $N_{wc} \approx 1.0 - 1.5 \times 10^{20} D m^{-2}$, so for f deuterium atoms accepted per wall-surface particle, then approximately $J \sim (N_{wc}/f) (V_m/N_A)^{2/3} \approx 6/f$ monolayers are able to participate in pumping during a discharge, where $V_m = (V_m^C + V_m^B)/2$ (m^3) is the mean molar volume of C and B and N_A is Avogadro's number. This rather limited capacity would be an impediment to more prolonged plasmas on MAST, unless their density were kept low, or significantly more efficient fuelling methods (eg pellet injection) were employed, or both. Recall N_{wc} will also be reached more quickly if physically $(S/XB)^{D2} > (S/XB)^D$, since n_{D2} and associated wall fluxes are then higher for a given $\langle n_e \rangle$. However, an

which is superior in this respect to alternatives against \bar{n}_e , or Φ_{out} , or even with four degrees-of-freedom P_{tot} , I_p , V_p , Φ_{out} . This outcome is summarized in Fig.2, and strongly suggests tank-gas density is the dominant factor affecting majority-particle confinement on MAST. Also superimposed are 6 sample discharges repeated with the contrasting assumption^[4] $(S/XB)^{D2} = 40$. Although n_{D2} is necessarily raised and τ_i lowered in each instance, the same trend is remarkably well preserved. Accompanying estimates of τ_E from EFIT reconstruction, shown too, in turn point towards a similar decrease for higher values of n_{D2} .

in-vessel divertor with closure and cryopumping will be installed in a future upgrade of MAST, providing for pumping and plasma density control^[1] which practically will never degrade.

4. Conclusions

Interpretative global modelling of majority-particle balance on MAST suggests core confinement time τ_i varies inversely with outboard gas-puffing rate, being higher when Φ_{out} is lower, and vice versa. In addition, steady-state τ_i is governed chiefly by surrounding molecular density n_{D_2} in the large vacuum tank, $\tau_i \propto n_{\text{D}_2}^{-0.7}$, irrespective of configuration or heating scheme. Such susceptibility is close to expectations for constant core fuelling efficiency e_1 as construed, plus roughly constant content N_i , since $\partial N_i / \partial t \approx 0 \Rightarrow N_i / \tau_i \approx e_1 S \propto n_{\text{D}_2}$. The large alteration in τ_i inferred (Fig.2), which is much greater than modelling uncertainties, therefore probably does reflect a genuine change in particle behaviour, viz ion efflux tends to rise for a given $\langle n_e \rangle$ with stronger fuelling from the surrounding gas envelope. A similar trend is hinted by estimated energy confinement time, at least for higher values of n_{D_2} . This emphasizes the importance of minimizing tank-gas density to optimize performance, something which can be accomplished for a given steady plasma density only by improving core fuelling efficiency^[1] (and not by stronger pumping), eg using inboard puffing, or ideally deep pellet injection. The main qualification is that so far n_{D_2} has only been calculated. Measurements during MAST pulses will become available with a screened fast ionization gauge, now being implemented. The wide variation in n_{D_2} already predicted for existing conditions (Fig.2) will be checked, helping to verify the global model and to resolve D α emission by molecules (“S/XB”)^{D2}. Maximum inventory of wall pumping will also be confirmed. Longer term, plasma density control in sustained high-density discharges will be ensured by supplementing limited wall sinks with a closed, cryopumped divertor.

References

- [1] G P Maddison, A Turner, S J Fielding & S You, Plasma Phys Control Fusion **48** (2006) 71
- [2] A R Field *et al*, Nucl Fusion **36** (1996) 119
- [3] S Brezinsek *et al*, Plasma Phys Control Fusion **47** (2005) 615
- [4] S J Fielding *et al*, J Nucl Mater **128 - 129** (1984) 390

This work was funded jointly by the United Kingdom Engineering and Physical Sciences Research Council and by the European Communities under the contract of Association between EURATOM and UKAEA. The views and opinions expressed herein do not necessarily reflect those of the European Commission.

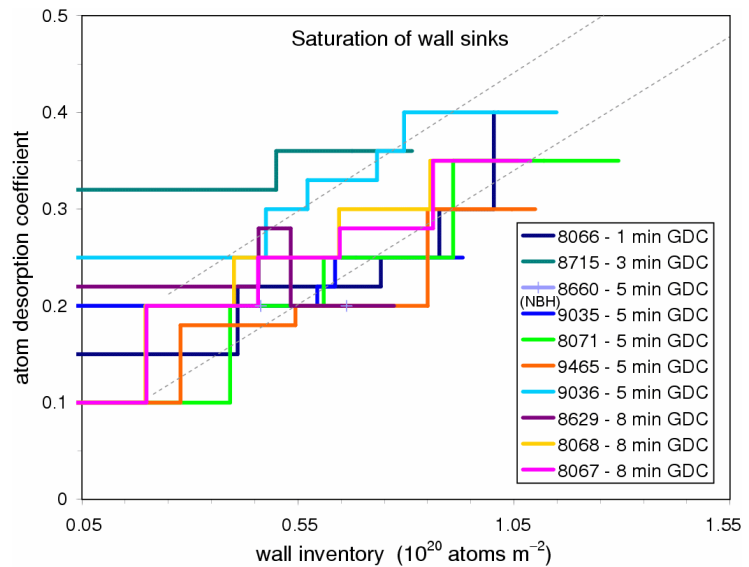


Fig.3 Calculated rise of wall desorption with adsorbed inventory for selected cases (all DND, sorted by prior GDC / plasma density). Dashed lines added for guidance.